sciendo Applied Mathematics and Nonlinear Sciences 5(1) (2020) 35–46

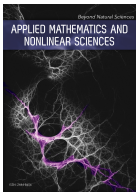

Applied Mathematics and Nonlinear Sciences

https://www.sciendo.com

Finite-time active disturbance rejection control for marine diesel engine

Yuanqing Wang[a,b†], Guichen Zhang[a], Zhubing Shi[b], Qi Wang[b], Juan Su[b], Hongyu Qiao[b]

a. Merchant Marine College, Shanghai Maritime University, Shanghai 201306, China

b. Marine Engineering Department, Nantong Shipping College, Nantong 226010, China

Submission Info

Communicated by Juan Luis Garcıa Guirao
Received November 12th 2019
Accepted January 14th 2020
Available online February 28th 2020

Abstract

In order to handle the non-linear system and the complex disturbance in marine engines, a finite-time convergence active disturbance rejection control (ADRC) technique is developed for the control of engine speed. First, a model for the relationship between engine speed and fuel injection is established on the basis of the mean value engine model. Then, to deal with the load disturbances and model parameter perturbation of the diesel engine, this paper designs an ADRC approach to achieve finite-time stability. Finally, simulation experiments show that the proposed method has better control effect and stronger disturbance rejection ability in comparison with the standard linear ADRC.

Keywords: non-linear system, marine engine, finite time, active disturbance rejection control.
AMS 2010 codes: 45G15

1 Introduction

Marine diesel engines are widely used in the domain of ship propulsion [1, 2]. The most crucial task is to have a reliable control system to regulate its speed for safe and efficient operation under the inherent instabilities and disturbances, coupled with the unpredictable external environment [3]. With the development of control technology and the requirement for dynamic positioning systems, several control methods have been already applied [4]. These methods can be mainly divided into two categories, namely, the model-based control methods and the optimisation-based black box methods [5]. The model-based control methods usually include optimal control [6], adaptive control [7], sliding mode control [8] and so on. These methods need to obtain an accurate mathematical model. The performance of model-based control methods greatly depends on the accuracy of the model, but it is hard to achieve in practice. By contrast, the optimisation-based black box methods usually include the classic proportional–integral–derivative (PID) control [9], fuzzy control [10], active disturbance

†Corresponding author.
Email address: wangyqdmu@163.com

sciendo ISSN 2444-8656 doi:10.2478/AMNS.2020.1.00004 sciendo

rejection control (ADRC) [11], modeless control and so on. These methods can achieve a good control effect without an accurate mathematical system model.

For the speed controller of a marine engine, the main task is to deal with the uncertain disturbances and the adjustment of system parameters. To handle uncertain disturbances, the ADRC method has introduced an extended state observer (ESO) in the feedback loop to compensate for the unmeasured states and the disturbances at the same time [12–14]. In addition to ADRC, the ESO can also be combined with other control methods to deal with uncertain disturbances and be simplified into a linear ESO (LESO) [15,16] for easier parameter adjustment [17]. Although simplification of both the control structure and the bandwidth tuning method facilitates the application of the LESO, non-linear ESO has been rarely studied [18, 19]. Therefore, it is essential to further study the non-linear ESO.

On the other hand, due to its advantages in terms of faster convergence rates, higher accuracies and better disturbance rejection properties, finite-time stability is also an important demand for control systems, especially in practice [20,21]. However, as far as our knowledge goes, the finite-time stabilisation of ADRC has never been attempted in the literature before.

In this paper, a novel ADRC law is proposed for a class of uncertain non-linear systems. The considered system uncertainties arise from the possibly unknown system dynamics, external disturbance and the parameter mismatch of control. To stay close to the basic concept of ADRC, the total uncertainties are treated as an extended state of the plant and are then estimated via non-linear ESO; finally, we compensate for these in the control action, in real time. Based on the output of the ESO, a finite-time sliding mode controller is designed [22]. A switching function is also defined to guarantee that the proposed control law is continuously differentiable. Theoretical analysis based on the Lyapunov stability theory show that the origin of the closed loop is semi-global finite-time stable.

The remainder of this paper is organised as follows. The mathematic model for the speed of a marine diesel engine is introduced in the section ‘Marine diesel engine speed model’. In the section titled ‘ADRC design’, we use an inverse hyperbolic sine function to design a non-linear ESO for the diesel engine speed model. The new non-linear ESO method, which has few adjustment parameters, is proposed to achieve precise control of marine diesel engine speed under uncertain disturbances. We design a finite-time sliding mode controller for ADRC (FT-SADRC), and it is proved that the controller can converge in finite time. In the section ‘Simulation experiments’, several experiments are carried out under the conditions of random load disturbances, manoeuvring the operations respectively, and the performance of the new ADRC method is verified in comparison to the linear ADRC (LADRC) method. In the ‘Conclusion’ section, conclusions and future research directions are presented.

2 Model for speed of marine diesel engine

In this paper, the electronically controlled diesel engine 7RT-Flex60C is studied. The maximum sustained power is 16520 kW, and the rated speed is 114 r/min. The relationship between the input (fuel injection) and the output (speed) of the diesel engine is obtained from the mean value engine model [23], which is adopted in this article.

$$\frac{\mathrm{d}n_{\mathrm{e}}}{\mathrm{d}t} = -\frac{10^3 V_{\mathrm{d}}(k_1 n_{\mathrm{e}} + k_2 {n_{\mathrm{e}}}^2)}{N_{\mathrm{st}} I}\frac{30}{\pi^2} - \frac{K_{\mathrm{Q}}\rho {n_{\mathrm{e}}}^2 D^5}{I}\frac{30}{\pi} + (\frac{30}{\pi})^2 \frac{10^3 \eta_{\mathrm{i}} H_{\mathrm{u}} \dot{m}_{\mathrm{f}}}{n_{\mathrm{e}} I}, \tag{1}$$

where V_d is the volume of air cylinder per cycle; k_1 and k_2 are the coefficients of the fitting function; N_{st} is the number of strokes; K_Q is the torque coefficient; ρ is seawater density; D is the diameter of the propeller; η_{i} indicates the thermal efficiency; I is the total moment of inertia of the diesel engine, shaft system and propeller; H_u is the lower heat value of the fuel; $\dot{m}_f$ is the average mass of fuel flowing into the cylinder per cycle; and $n_{\mathrm{e}}(t)$ is the diesel engine speed. Suppose $u = \dot{m}_f$, $f(n_{\mathrm{e}}(t)) = -\frac{10^3 V_{\mathrm{d}}(k_1 n_{\mathrm{e}}(t) + k_2 n_{\mathrm{e}}(t)^2)}{N_{\mathrm{st}} I}\frac{30}{(\pi)^2} - \frac{K_{\mathrm{Q}}\rho n_{\mathrm{e}}(t)^2 D^5}{I}\frac{30}{\pi}$ and $g(n_{\mathrm{e}}(t)) = \left(\frac{30}{\pi}\right)^2 \frac{10^3 \eta_{\mathrm{t}} H_{\mathrm{u}}}{n_{\mathrm{e}}(t) I}$; then, Eq. (1) can be expressed as $\frac{\mathrm{d}n_{\mathrm{e}}}{\mathrm{d}t} = f(n_{\mathrm{e}}) + g(n_{\mathrm{e}})u$.

We define the following functions:$x_1(t) = \int n_e(t)dt$;$x_2(t) = n_e(t)$. Then, the second-order state-space model between the fuel injection and the speed of a diesel engine can be obtained as follows:

$$\begin{cases} \dot{x}_1(t) = x_2(t) \\ \dot{x}_2(t) = f(x_1(t), x_2(t)) + g(x_1(t), x_2(t))u - b_0u(t) + b_0u(t) \\ y = x_2(t) \end{cases} \tag{2}$$

where $b_0 > 0$;$u(t)$ is the control input for the system; $y(t)$ is the system output.

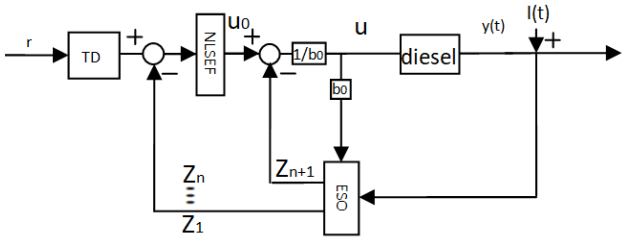

Fig. 1 The propulsion control system with load disturbances.

The load perturbation of the diesel engine is the disturbance caused by complex sea conditions. The ADRC system with load disturbance characteristics is shown in Fig. 1.

According to the working principle of Fig. 1, the marine diesel engine propulsion control system with load disturbance can be expressed as follows:

$$\begin{cases} \dot{x}_1(t) = x_2(t) \\ \dot{x}_2(t) = f(x_1(t), x_2(t)) + g(x_1(t), x_2(t))u(t) - b_0u(t) + b_0u(t) + l(t) \\ y = x_2(t) \end{cases} \tag{3}$$

where $l(t)$ is the system's load disturbance, $|l(t)| < L$ and L is a constant. Here, $f(x_1(t), x_2(t)) + g(x_1(t), x_2(t))u(t) - b_0u(t) + l(t)$ is the new lumped disturbance, and it is bounded. We define $x_3(t) = f(x_1(t), x_2(t)) + g(x_1(t), x_2(t))u(t) - b_0u(t) + l(t)$ as the extended state, and suppose $\dot{x}_3 = o(t)$. Then, Eq. (3) is extended as in Eq. (4):

$$\begin{cases} \dot{x}_1(t) = x_2(t) \\ \dot{x}_2(t) = x_3(t) + b_0u(t) \\ \dot{x}_3(t) = o(t) \\ y = x_2(t) \end{cases} \tag{4}$$

3 Controller design

The ADRC approach consists of three modules: tracking differentiator (TD), ESO and the non-linear state error feedback (NLSEF) control [24]. The TD generates a transient trajectory to avoid the set point jump. The system's total disturbance is estimated by the ESO. The NLSEF is a non-linear PID controller.

The modules' design is independent. Each module can be designed separately according to the controlled object and combined together to acquire the ADRC controller. For the system represented by Eq. (4), the TD in discrete form is as follows:

$$\begin{cases} \dot{v}_1(t) = v_2(t) \\ \dot{v}_2(t) = R^2\{-a_1 |e_1| arsh(e_1) - a_2 |e_2| arsh(e_2/R)\} \end{cases} \tag{5}$$

where $arsh()$ is an inverse hyperbolic sine function $\left(arsh(x) = \ln\left(x + \sqrt{x^2+1}\right)\right)$ [25]; $e_1(t) = \int e_2(t)dt$, $e_2(t) = v_2(t) - r(t)$; $r(t)$ is the system's reference signal; R>0, a_1>0 and a_2>0. For any bounded integrable function

$r(t)$, the tracking value of $r(t)$ is $v_2(t)$, which satisfies Eq. (6):

$$\lim_{R\to\infty}\int_0^T |v_2(t)-r(t)|\,dt = 0 \tag{6}$$

where $T>0$. The ESO is selected as follows:

$$\begin{cases} e_3(t) = z_1(t) - \int_0^t y(t)dt \\ \dot{z}_1(t) = z_2(t) - \beta_1 e_3(t) \\ \dot{z}_2(t) = z_3(t) - \beta_2 \cdot arsh(e_3(t)) + b_0 u(t) \\ \dot{z}_3(t) = -\beta_3 \cdot arsh(e_3(t)) \end{cases} \tag{7}$$

where $\beta_1 > 0$, $\beta_2 > 0$ and $\beta_3 > 0$; $z_1(t)$ and $z_2(t)$ track the output variables $x_1(t)$ and $x_2(t)$, respectively; and $x_3(t)$ is the extended state and is used to estimate the total disturbance. For the ESO, the method of parameter tuning is used and described as follows:

$$\beta_1 = 9v_{\text{eso}}, \beta_2 = 27v_{\text{eso}}^2, \beta_3 = 27v_{\text{eso}}^3 \tag{8}$$

where $v_{\text{eso}}$is the observer observation speed. Because $\beta_1\beta_2 - \beta_3 = 243v_{\text{eso}}^3 - 27v_{\text{eso}}^3$ and $\omega_{\text{eso}} > 0$, the stability condition of the observer can be satisfied [26]: $\beta_1\beta_2 - \beta_3 > 0$.

In order to improve the control performance, we apply the sliding mode error feedback control law to the ADRC. We define the following: $e_6(t) = \int e_7(t)dt$, and $e_7(t) = y(t) - r = x_2(t) - r$. Here, r is the system's reference signal. And hence, the error system corresponding to Eq. (4) is

$$\begin{cases} \dot{e}_6(t) = e_7(t) \\ \dot{e}_7(t) = f(x_1(t),x_2(t)) + g(x_1(t),x_2(t))u(t) - b_0u(t) + b_0u(t) + l(t) \end{cases} \tag{9}$$

We know that $u(t) = (u_0(t) - z_3(t))/b_0$ [27]; the system represented in Eq. (9) can be rewritten as follows:

$$\begin{cases} \dot{e}_6(t) = e_7(t) \\ \dot{e}_7(t) = f(x_1(t),x_2(t)) + g(x_1(t),x_2(t))u(t) - b_0u(t) + b_0u(t) + l(t) + u_0(t) - z_3(t) \end{cases} \tag{10}$$

Due to the expansion of the observer convergence in Eq. (7), i.e. $z_1(t) \to x_1(t)$, $z_2(t) \to x_2(t)$ and $z_3(t) \to$ $x_3(t) = f(x_1(t),x_2(t)) + g(x_1(t),x_2(t))u(t) - b_0u(t) + l(t)$, the system represented in Eq. (10) can be rewritten as follows:

$$\begin{cases} \dot{e}_6(t) = e_7(t) \\ \dot{e}_7(t) = u_0(t) \end{cases} \tag{11}$$

And then, we introduce the following lemma, which is useful in the paper.

Consider the following non-linear systems [28]:

$$\dot{x} = f(x), x \subseteq R^n, f(0) = 0 \tag{12}$$

where $f : D \to R^n$ satisfies the locally Lipschitz continuous condition and $x = [x_1, x_2 \cdots x_n]^T$ represents the state.

Lemma 1 [28]: Consider the non-linear system, Eq. (12); suppose that there exist any real numbers $k>0$ and $0<\alpha<1$; also, $\alpha \in C^1$ function $V(x)$, which is defined in a neighbourhood $\widehat{U} \subset U_0 \subset R^n$ of the origin, such that $V(x)$ is positive definite on $\widehat{U}$ and $\dot{V}(x) + cV^a(x)$ is negative semi-definite on $\widehat{U}$; then, the origin of system represented by Eq. (4) is finite-time stable. The settling time depends on the initial state $x(0) = x_0$, and its upper bound is $T_x(x_0) \le \frac{V^{1-a}(x_0)}{c(1-a)}$,

$$T_x(x_0) \le \frac{V^{1-a}(x_0)}{c(1-a)},$$

where x_0 is in an open neighbourhood of the origin x=0. The origin of the system represented by Eq. (20) is globally finite-time stable if $\widehat{U} = R^n$ and $V(x)$ is radially unbounded, i.e. when $\|x\| \to +\infty$ and $V(x) \to +\infty$.
In the following section, the finite-time stability theory is used to analyse the convergence of the sliding mode error feedback control.
Based on the finite-time convergence stability theory and the sliding-mode control theory, we can design a controller for the finite-time convergence of the guidance system represented by Eq. (11) and give the following result.
Definition 1: Consider the system represented by Eq. (4); we design the system control quantity in the form of Eq. (15).

$$u(t) = \frac{1}{b_0}(-z_3(t) - k_1\gamma|e_6(t)|^{\gamma-1} - \frac{a}{R}\mathrm{sgn}(s)|s|^{\eta}) \tag{13}$$

where $0 < \gamma < 1$, $k_1 > 0$, $\alpha > 0$ and $\eta > 0$. Then, the state error $e_6(t), e_7(t)$ of the control system converges to zero in finite time, the diesel engine speed $x_2(t)$ converges to *r,* and the finite convergence time of the control system is satisfied by Eq. (21):

$$T_H \leq \frac{R_0 S^{(1-\eta)}(0)}{a(1-\eta)} + \frac{S^{(1-\gamma)}(0)}{k_1(1-\gamma)} \tag{14}$$

Proof:
The sliding surface of the system can be chosen as follows [29]:

$$S = e_7(\mathrm{t}) + \mathrm{k}_1|e_6(t)|^{\gamma}\mathrm{sgn}(e_6(t)) \tag{15}$$

where $0 < \gamma < 1$ and $k_1 > 0$.

According to the reaching condition of sliding-mode control, $S\dot{S} \leq 0$, we design the reaching law as follows:

$$\dot{S} = -\frac{a\mathrm{sgn}(S)}{R}|S|\,\eta, a > 0, \eta > 0 \tag{16}$$

where $R = |e_7|$, $0 < R < R_0$ and $R_0 = r$.

From Eqs (15) and (16), we have

$$S\dot{S} = -\frac{a}{R}|S|^{\eta+1} < 0 \tag{17}$$

Equation (17) shows that the system meets the reaching condition, i.e. the system's state can reach the sliding mode surface.

We take the derivative of Eq. (15) and then connect Eq. (11) and Eq. (16):

$$\begin{aligned} u(t) &= \tfrac{1}{b_0}(-f(x_1(t),x_2(t)) - g(x_1(t),x_2(t))u(t) + b_0u(t) - l(t) - k_1\gamma|e_6(t)|^{\gamma-1}e_7(t) - \tfrac{\alpha}{R}\mathrm{sgn}(s)|s|^{\eta}) \\ &= \tfrac{1}{b_0}(-z_3(t) - k_1\gamma|e_6(t)|^{\gamma-1}e_7(t) - \tfrac{\alpha}{R}\mathrm{sgn}(s)|s|^{\eta}) \end{aligned} \tag{18}$$

We selected the non-linear control law as follows:

$$u_0 = -k_1\gamma|e_6(t)|^{\gamma-1}e_7(t) - \frac{\alpha}{R}\mathrm{sgn}(s)|s|^{\eta} \tag{19}$$

Therefore, the control input can be obtained as follows:

$$u(t) = \frac{1}{b_0}(-z_3(t) - u_0(t)) \tag{20}$$

Next, we analyse the convergent property of the system based on the finite-time convergence stability theory. The motion of the state can be divided into two stages: (i) the approaching stage; and (ii) the sliding state.

For the approaching stage, the Lyapunov function can be chosen as follows:

$$V = S^2 \tag{21}$$

The derivative of V along the trajectories of Eq. (21) satisfies the following relation:

$$\dot{V} = 2S\dot{S} \tag{22}$$

From Eqs (11) and (22), we have

$$\dot{V} = -2\frac{a}{R}|S|^{\eta+1} < 0 \tag{23}$$

From Eqs (21) and (23), we have

$$\dot{V} = -2\frac{a}{R}V^{\frac{1}{2}(\eta+1)} \tag{24}$$

Consider the operation of the control system, $R = |e_7(t)|$, $0 < R < R_0, R_0 = r$ and $R_0 = r$.
Therefore,

$$\dot{V} = -2\frac{a}{R}V^{\frac{1}{2}(\eta+1)}, \forall t > 0 \tag{25}$$

According to Lemma 1, the state will converge to the sliding surface in a finite time. The convergent time satisfies the following:

$$T_1 \leq \frac{R_0 V^{\frac{1}{2}(1-\eta)}(0)}{a(1-\eta)} = \frac{R_0 S^{(1-\eta)}(0)}{a(1-\eta)} \tag{26}$$

After arriving at the sliding mode surface, the system will move along the surface until it converges to zero. So, the state meets the following requirements:

$$S = e_7(\mathrm{t}) + k_1|e_6(t)|^{\gamma}\mathrm{sgn}(e_6(t)) = 0 \tag{27}$$

Consider that

$$\dot{e}_6(t) = e_7(t) \tag{28}$$

And hence, from Eqs (27) and (28), we have

$$e_6 = k_1|e_6(t)|^{\gamma}\mathrm{sgn}(e_6(t)) \tag{29}$$

We define that

$$e_6 = S \tag{30}$$

Equation (29) can be written as

$$S' = k_1\left|S'\right|^{\gamma}\mathrm{sgn}(S') \tag{31}$$

Choose the Lyapunov function for Eq. (31) as follows:

$$V' = S'^2 \tag{32}$$

And then, we have the following time derivative of V':

$$\dot{V}' = 2S'\dot{S}' \tag{33}$$

From Eqs (30) and (31), we have

$$\dot{V}' = 2k_1\left|S'\right|^{\gamma+1} \leq 0 \tag{34}$$

According to Lemma 1, the convergent time of the system represented by Eq. (31) satisfies the following:

$$T_2 \leq \frac{V^{\frac{1}{2}(1-\gamma)}(0)}{k_1(1-\gamma)} = \frac{S'^{(1-\gamma)}(0)}{k_1(1-\gamma)} \tag{35}$$

Table 1 Parameters of the RT-Flex60C engine

Parameters	Value
Number of cylinders	7
Stroke	2250 mm
Crank link ratio	0.489
Compression ratio	18.4
Stroke number	2
Cylinder diameter	600 mm
Rated speed	114 r/min
Rated power	16520 kW
Rated torque	1390 kN·m
Specific fuel consumption	177 g/kWh

Therefore, the whole convergent time of the control system can be given as follows:

$$T_H \leq T_1 + T_2 \leq T_1 \leq \frac{R_0 S^{(1-\eta)}(0)}{a(1-\eta)} + \frac{S'^{(1-\gamma)}(0)}{k_1(1-\gamma)} \tag{36}$$

So, the control system is finite-time convergent.

Remark 1 From Eq. (36), we can know that the convergent time relates to the parameters a, k_1, γ; so, we can control the convergent rate by adjusting the parameters.

Remark 2 In this paper, we use the sine function $arsh(S)$ instead of the sign function $sgn(S)$. Because it is a smooth function, the control process is stable, and the control precision is improved.

4 Simulation study

In order to verify the effectiveness of the proposed FT-SADRC, the RT-Flex60C low-speed two-stroke marine diesel engine, which is installed on the container ship of Orient Overseas International Limited (OOIL), is chosen for the simulation experiments. The main parameters of the RT-Flex60C engine are shown in Table 1.

To make a comprehensive analysis of the control performance of the proposed FT-SADRC method, a standard LADRC method is used to conduct the comparison. The robustness of the control algorithm under the conditions of a random disturbance load and sudden load dumping needs to be verified.

4.1 Random disturbance load

During the actual navigation, the wind and the waves have an effect on the propeller load, which are represented as random disturbances. In this test, random disturbances with an amplitude of $25 \times 10^3 \sin(t \cdot 20\pi)$ Nm are set as external disturbances, the simulation time is set to 10 s and the initial speed of the diesel engine is the rated speed 114 r/min. In the process, the load torque of the propeller is 1390 kN·m. At 5 s, the load torque was suddenly reduced to 900 kN·m to simulate the propeller load change due to the wind and the waves.

Gao [17] proposed a tuning method based on the observer bandwidth for LADRC. In this test, the bandwidth of the observer ω_0=37, and the bandwidth of the controller $\omega_c = 3.5$.

The FT-SADRC parameter is selected as follows: R=10, b_0=1000, $v_{\text{eso}} = 2$, k_1=0.6, γ=0.8 and a=0.4.

The control results of the proposed FT-SADRC and the LADRC with random disturbances are shown in Figs 2 and 3. The following points can be noted:

(1) Although the control performances of both the methods are good, the tracking error of the FT-SADRC is much less than that of the LADRC. Furthermore, the tracking error of the FT-SADRC and the LADRC are 0.559 and 1.785r/min, respectively.

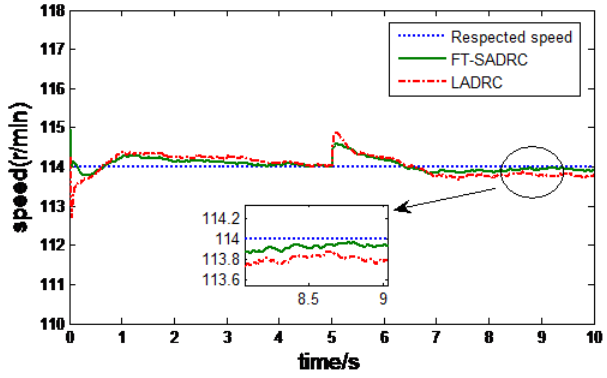

Fig. 2 Curve for the diesel engine speed y.

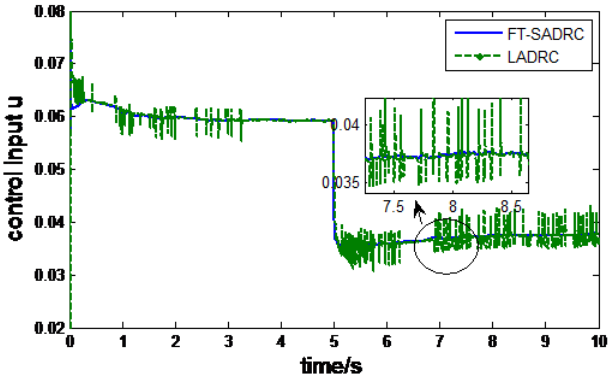

Fig. 3 Curve for the diesel engine control input u.

(2) In Fig. 3, we find that control input fluctuation is smaller for the FT-SADRC, which can save energy and reduce actuator wear.

4.2 Motor sailing analysis

This section describes the simulation analysis of the ship manoeuver navigation when entering and leaving a port. In this test, random disturbances with an amplitude of $25 \times 10^3 \sin(t \cdot 20\pi)$ Nm are set as external disturbances, the simulation time is set to 10 s and the initial speed of the diesel engine is the rated speed 114 r/min. In the process, the load torque of the propeller is 1390 kN·m. At 5 s, the diesel speed was changed to 90.5 r/min.

For the LADRC [27], the bandwidth of the observer ω_0=43, and the bandwidth of the control $\omega_c = 4.1$. The FT-SADRC parameter is selected as follows: R=10, b_0=1000, $v_{\text{eso}} = 2.7$, k_1=0.4, γ=0.9 and a=0.5.

It can be observed from the results in Fig. 4 that the maximum speed of the proposed FT-SADRC method is less than that of the LADRC method, and the time required to restore normal speed is also less than that of the LADRC method.

Moreover, it can be seen from Fig. 5 that the control input of FT-SADRC requires only about 0.5 s from the sudden load dumping to restore stability, while the LADRC requires >1 s. Therefore, the adjustment speed of the control input of the proposed method is faster than that of the LADRC.

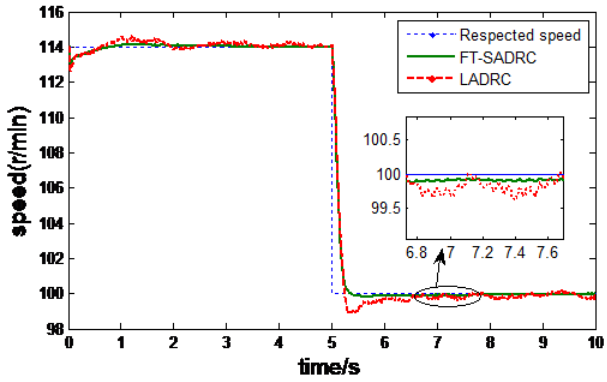

Fig. 4 Curve for the diesel engine speed y.

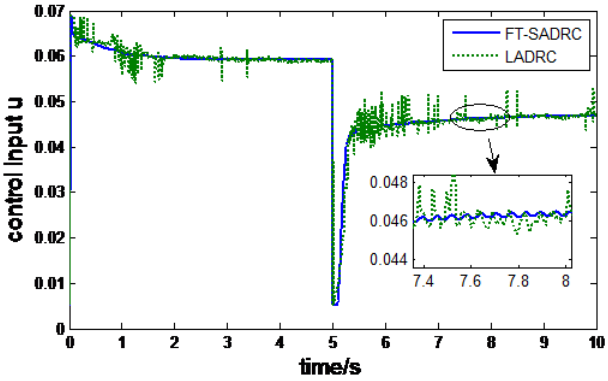

Fig. 5 Curve for the diesel engine control input u.

5 Conclusions

In the context of the marine diesel engine speed control problem under the random load disturbances and unknown uncertainties, the sliding-mode control method is put forward by combining a new ESO (based on the inverse hyperbolic sine function). Although the new observer is non-linear, the adjustment parameters are the same as for linear ESO, which reduces the difficulty in the application of the non-linear observer. The control law is constructed by sliding-mode control for ADRC, and the method can achieve finite-time convergence and improve the convergence speed and control precision. From the simulation experiment using the model of a large, low-speed two-stroke marine diesel engine RT-Flex60c, we can observe that the proposed method has more advantages than the LADRC method, such as control accuracy and disturbance rejection (both random disturbance and sudden load dumping disturbance).

Thus, the main contributions of this article are summarised as follows. (1) In theory, a new ESO and finite-time convergence control law is proposed, which makes full use of the known non-linear term in the diesel engine model and further improves the adaptability of the controller. The proposed method can be applied to control issues of other systems that have known non-linear terms. (2) In practice, the proposed method can maintain smoother, quicker regulation, with fewer tuning parameters of the diesel engine speed under different external and system disturbances and has more practical significance compared with LADRC. Actually, the fuel injection signal of a marine diesel engine is usually maintained at several fixed positions for safety and economy. Therefore, the proposed method under a certain output constraint could be considered further.

Acknowledgement: This work was supported by the National Natural Science Foundation of China (51779136), the Natural Science Foundation of the Higher Education Institutions of Jiangsu Province, China (18KJB413008)

and the Natural Science Foundation of Jiangsu Province (BK20191205).

References

[1] Du B, Wu S, Han S, et al. Application of linear active disturbance rejection controller for sensorless control of internal permanent-magnet synchronous motor. IEEE Transactions on Industrial Electronics, 2016, 63(5): 3019-3027.
[2] Xie S, Chu X, Liu C, et al. Marine diesel engine speed control based on adaptive state-compensate extended state observer-backstepping method. Proceedings of the Institution of Mechanical Engineers, Part I: Journal of Systems and Control Engineering, 2019, 233(5): 457-471.
[3] TANG J, LEI Y, NIE G, et al. Application of PID neural network in control of diesel engine speed. Coal Mine Machinery, 2010, 1: 201-204.
[4] Bø T I, Johansen T A, Sørensen A J, et al. Dynamic consequence analysis of marine electric power plant in dynamic positioning. Applied Ocean Research, 2016, 57: 30-39.
[5] Yan X, Xu L, Wang Y. The Loading Control Strategy of the Mobile Dynamometer Vehicle Based on Neural Network PID. Mathematical Problems in Engineering, 2017.
[6] Bryson A E. Applied optimal control: optimization, estimation and control. Routledge, 2018.
[7] Liu Y J, Lu S, Tong S, et al. Adaptive control-based barrier Lyapunov functions for a class of stochastic nonlinear systems with full state constraints. Automatica, 2018, 87: 83-93.
[8] Utkin V, Guldner J, Shi J. Sliding mode control in electro-mechanical systems. CRC press, 2017.
[9] Cui W, Guo R, Fan D. Application of Neural Network PID Control in Hump Pushing Peak Process. DEStech Transactions on Computer Science and Engineering, 2017 (icitia).
[10] El-Samahy A A, Shamseldin M A. Brushless DC motor tracking control using self-tuning fuzzy PID control and model reference adaptive control. Ain Shams Engineering Journal, 2018, 9(3): 341-352.
[11] Wang R, Li X, Liu Y, et al. Variable Sampling Rate based Active Disturbance Control for a Marine Diesel Engine. Electronics, 2019, 8(4): 370.
[12] Wang F, Guo Y, Wang K, et al. Disturbance observer based robust backstepping control design of flexible air-breathing hypersonic vehicle. IET Control Theory & Applications, 2019, 13(4): 572-583.
[13] Wu Z, He T, Li D, et al. Superheated steam temperature control based on modified active disturbance rejection control. Control Engineering Practice, 2019, 83: 83-97.
[14] Tavasoli A. Active disturbance rejection boundary control of Timoshenko beam with tip mass. ISA transactions, 2018, 80: 221-231.
[15] Castillo A, García P, Sanz R, et al. Enhanced extended state observer-based control for systems with mismatched uncertainties and disturbances. ISA transactions, 2018, 73: 1-10.
[16] Zheng Q, Ping Z, Soares S, et al. An Active Disturbance Rejection Control Approach to Fan Control in Servers. IEEE Conference on Control Technology and Applications (CCTA). IEEE, 2018: 294-299.
[17] Gao Z. Scaling and bandwidth-parameterization based controller tuning. In: Proceedings of the American control conference, Denver, CO, 4–6 June 2003, pp.4989–4996.New York: IEEE.
[18] Wang R, Li X, Zhang J, et al. Speed control for a marine diesel engine based on the combined linear-nonlinear active disturbance rejection control. Mathematical Problems in Engineering, 2018, 2018.
[19] Wang R, Li X, Liu Y, et al. Variable Sampling Rate based Active Disturbance Control for a Marine Diesel Engine. Electronics, 2019, 8(4): 370.
[20] Li T, Yang J, Wen C, et al. Global adaptive finite-time stabilization of uncertain time-varying p-normal nonlinear systems without homogeneous growth nonlinearity restriction. IEEE Transactions on Automatic Control, 2019.
[21] Zhang X, Li X, Cao J, et al. Design of memory controllers for finite-time stabilization of delayed neural networks with uncertainty. Journal of the Franklin Institute, 2018, 355(13): 5394-5413.
[22] Wu K N, Sun H X, Shi P, et al. Finite-time boundary stabilization of reaction-diffusion systems. International Journal of Robust and Nonlinear Control, 2018, 28(5): 1641-1652.
[23] Theotokatos G, Guan C, Chen H, et al. Development of an extended mean value engine model for predicting the marine two-stroke engine operation at varying settings. Energy, 2018, 143: 533-545.
[24] Huang Z, Liu Y, Zheng H, et al. A self-searching optimal ADRC for the pitch angle control of an underwater thermal glider in the vertical plane motion. Ocean Engineering, 2018, 159: 98-111.
[25] Bellemare M F, Wichman C J. Elasticities and the inverse hyperbolic sine transformation. Working Paper. University of Minnesota, 2018.
[26] Chen L, Chen G, Wu R, et al. Stabilization of uncertain multi-order fractional systems based on the extended state observer. Asian Journal of Control, 2018, 20(3): 1263-1273.
[27] Sira-Ramírez H, Zurita-Bustamante E W, Huang C. Equivalence Among Flat Filters, Dirty Derivative-Based PID Controllers, ADRC, and Integral Reconstructor-Based Sliding Mode Control. IEEE Transactions on Control Systems Technology, 2019.

[28] Bhat, S., Bernsein, D.: Lyapunov analysis of finite-time differential equations. In: Proceedings of the American Control Conference, pp. 1831–1832 (1995).
[29] Galván-Guerra R, Fridman L, Iriarte R, et al. Integral sliding-mode observation and control for switched uncertain linear time invariant systems: A robustifying strategy. Asian Journal of Control, 2018, 20(4): 1551-1565.